ANTICANCER RESEARCH *39*: 1785-1793 (2019)
doi:10.21873/anticanres.13285

Delivery of Antisense Oligonucleotide LOR-2501 Using Transferrin-conjugated Polyethylenimine-based Lipid Nanoparticle

BIN ZHENG[1], SHUANG YANG[2], QINGPING TIAN[1], YIN XIE[1], SHUQIU ZHANG[1] and ROBERT J. LEE[3,4]

[1]*School of Pharmacy, Shanxi Medical University, Taiyuan, P.R. China;*
[2]*School of Basic Medical Sciences, Shanxi Medical University, Taiyuan, P.R. China;*
[3]*College of Life Science, Jilin University, Changchun, P.R. China;*
[4]*College of Pharmacy, The Ohio State University, Columbus, OH, U.S.A.*

Abstract. *Background/Aim: Efficient delivery of antisense oligonucleotide (ASO) by nanoparticle vectors is critical for its clinical application. The aim of this study was to design and evaluate a novel ASO vector TPSH-LP consisting of a reduction-sensitive cationic polymer PEI-SS-HA (PSH), lipids and transferrin (Tf) as a targeting ligand. Materials and Methods: PSH was synthesized based on PEI 25 kDa. Nanoparticles containing PSH and Tf (TPSH-LP) were prepared and used to deliver an ASO LOR-2501 targeting ribonucleotide reductase R1. The physical and chemical properties of TPSH-LP and cellular uptake in HepG2 cells were studied. Results: TPSH-LP formed a complex with LOR-2501 (L-TPSH-LP) which showed suitable particle size (267.77±16.20 nm) and zeta potential (4.87±0.52 mV). TPSH-LP showed lower cytotoxicity and higher transfection efficiency than PEI 25 kDa in HepG2 cells. The addition of Tf enhanced the targeting and delivery efficiency of PSH-LP. TPSH-LP transported LOR-2501 and down-regulated the levels of R1 protein efficiently by 64.15%. Conclusion: Data demonstrated the potential utility of TPSH-LP for oligonucleotide delivery in cancer therapy.*

LOR-2501 is a 20-mer phosphorothioate antisense oligonucleotide (ASO) targeting ribonucleotide reductase R1 mRNA. However, ASOs have rapid clearance and show only a limited efficacy. Their clinical translation is limited, in part, by the lack of effective delivery vehicles (1-3). Nanoparticle vectors are promising as ASO delivery vehicles (4-5). The nanoparticles must be of appropriate size and zeta potential, have high biocompatibility, and be capable to release their contents into the cells (6-8).

Polyethylenimine (PEI) is a cationic polymer with high gene delivery activity (9). PEI has endosomolytic activity due to the "proton sponge" effect, which can facilitate intracellular ASO release. PEI 25 kDa is highly active, but has high cytotoxicity (10-11). Hydrophobic modification of PEI 25 kDa can improve its transfection activity and reduce its cytotoxicity. Reduced glutathione (GSH) is elevated inside the cell. Therefore, disulfide-based bioconjugates can be synthesized that are reduction-sensitive and break down intracellularly (12-14). Lipid nanoparticles (LPs) are also used in gene delivery (15-16). Combining modified PEI with LPs may produce further enhanced activity (17-19).

In this report, a novel reduction-sensitive cationic polymer based on PEI 25 kDa, named PEI-SS-HA was synthesized (Figure 1A). PEI-SS-HA was further combined with LPs and the ligand transferrin (Tf). Tf was added to the outermost layer of the LPs for the purpose of targeting the Tf receptor, which is overexpressed in tumor cells. The nanoparticles containing PEI-SS-HA and Tf were used to deliver an antisense oligo LOR-2501. The physical chemical properties and the cellular uptake in HepG2 cells were studied.

Materials and Methods

Materials. LOR-2501 (5'-CTC TAG CGT CTT AAA GCC GA-3') and 5'-Cy3-LOR-2501 were synthesized by Biomics Biotechnologies (Jiangsu, China). Egg phosphatidylcholine (ePC) and cholesterol were purchased from Avanti Polar Lipids, Inc. (Shanghai, China). Branched PEI 25kDa, hexadecylamine, Traut's Reagent (2-iminothiolane•HCl) and 3-(4,5-dimethylthiazol-2-yl)-2,5-diphenyl-tetrazolium bromide (MTT) were purchased from Sigma-Aldrich (St. Louis, MO, USA). SPDP was obtained from Dojindo (Dojindo Laboratory, Kumamoto, Japan). Dulbecco's modified Eagle's medium (DMEM), fetal bovine

Correspondence to: Robert J. Lee or Shuqiu Zhang, College of Life Science, Jilin University, No.2699, Qianjin Street, Changchun 130012, P.R. China; School of Pharmacy, Shanxi Medical University, No. 56 Xinjian South Road, Taiyuan 030001, P.R. China. Tel: +86 3513985243, e-mail: lee.1339@osu.edu or shuqiu.zhang@126.com

Key Words: Polyethylenimine, transferrin, lipid nanoparticles, oligonucleotide, cancer.

serum (FBS) and 0.25% (w/v) trypsin were purchased from HyClone (Logan, UT, USA). Succinimidyl 3-(2-pyridyldithio) propionate (SPDP) and 4',6-Diamidino-2-phenylindole (DAPI) was purchased from Thermo Fisher Scientific (Rockford, IL, USA). HepG2 cells were purchased from American Type Culture Collection (ATCC). All other analytical reagents were commercially obtained in reagent grade.

Synthesis of PEI-SS-HA. PEI-SS-HA was synthesized as described previously (20). Firstly, 0.8 μmol PEI 25 kDa and 20 μmol SPDP were dissolved into ethanol to achieve concentrations of 20 mg/ml and 100 mg/ml, respectively. The SPDP solution was added to the PEI 25 kDa solution rapidly under stirring. The mixture was incubated for 4h at room temperature (25˚C) to prepare the PEI-PDP solution. Then, 30 μmol hexadecylamine (HA) was dissolved in 1 ml ethanol, and 60 μmol Traut's Reagent (2-Iminothiolane•HCl) was dissolved into 0.5 ml water. The Traut's Reagent solution was added to the HA solution under stirring and the mixture was incubated for 3 h at room temperature (25˚C) in the dark, yielding HA-SH. Then, the HA-SH solution was added to the PEI-PDP solution slowly under vortex mixing. The reaction mixture was then stirred at room temperature (25˚C) for 4 h. Then, the product was transferred into a dialysis tube (MWCO 10 kDa) and dialyzed against deionized water for 24 h. Finally, the solution was freeze-dried to obtain PEI-SS-HA (PSH), with the structural formula shown in Figure 1A.

Cell culture. HepG2 cells were grown and propagated in Dulbecco's modified Eagle's medium (DMEM), supplemented with 10% FBS and 1% antibiotics (100 units/ml penicillin and 100 μg/ml streptomycin, Sigma). Cells were grown at 37˚C in a humidified atmosphere containing 5% CO_2.

Buffer capacity determination of PSH. To assess the buffering capacity of the synthetic polymer, the ability of PEI-SS-HA (PSH) to buffer from pH 10-2 was determined by acid-base titration (20-21). Firstly, 0.5 mg/ml PEI 25 kDa and PSH solutions were prepared. Then the pH of the solution was raised to 10 using 1 mol/l NaOH. Then, 0.1 mol/l HCl was added in 10 μl increments into 2 ml polymer solution. pH values were measured after stirring thoroughly. The curve of hydrochloric acid volume vs pH value was plotted.

Preparation and characterization of LPs. An ethanol dilution method was used for the preparation of LPs containing LOR-2501 (L-LPs) (22-24). Firstly, PEI-SS-HA (PSH), ePC and cholesterol were dissolved in ethanol at molar ratio 40/18/35. Then, the ethanolic lipid solution was injected into the PBS buffer (pH 6.8) under stirring at a ratio of 1/3 (v/v) to obtain LPs containing PSH (PSH-LP). LOR-2501 was separately dissolved in diethyl pyrocarbonate-treated water. To obtain LPs containing LOR-2501 (L-PSH-LP), the LOR-2501 solution was added into the PEI-SS-HA/lipid mixture and vortexed for 30 sec, at varying nitrogen-to-phosphate (N/P) ratios, ranging from 1:1 to 10:1. "N" represented the molarity of nitrogen in PEI or PSH, and "P" represented the molarity of phosphorus in LOR-2501. To prepare LPs containing transferrin (Tf), post-insertion was used. Tf-Chol was incubated with the PSH-LP or L-PSH-LP for 1 h at 37 ˚C at Tf-Chol/total lipid ratios from 1/60 to 1/140. The resulting LPs were named TPSH-LP and L-TPSH-LP. A schematic diagram of the preparation process of LPs is shown in Figure 1B. Finally, all the LPs were concentrated by ultrafiltration with a tubular polysulfone ultrafiltration membrane (MWCO 100 kDa).

The particle sizes and zeta potentials of L-PSH-LP and L-TPSH-LP at various N/P ratios or Tf-Chol/total lipid ratios were determined on a Zetasizer Nano ZS 90 instrument (Malvern Instruments, Ltd., Malvern, UK). Each data point was calculated averaging 3 measurements. The structure of L-TPSH-LP was investigated by field emission scanning electron microscope (FE-SEM) (JSM-6700F, JEOL, Tokyo, Japan). SEM images were taken at 3.0 kV accelerating voltage.

Gel retardation assay for determining complexes of LPs with PSH and TPSH. PEI 25 kDa, PSH-LP and TPSH-LP were combined with LOR-2501 to form L-PEI, L-PSH-LP and L-TPSH-LP. Two microliter of 6×sample buffer (50% glycerol, 1% bromophenol blue, and 1% xylene cyanol FF in Tris-borate EDTA (TAE) buffer) was added to each sample. The samples were loaded onto 3% agarose gel containing 0.2% mg/ml ethidium bromide, and the electrophoresis was run in TAE running buffer at 120 V for 20 min. The resulting gels were photographed under UV-illumination.

Cytotoxicity assay. HepG2 cells were seeded at a density of 1×10^4 cells/well in a 96-well plate and cultured for 24 h in 100 μl DMEM containing 10% FBS. Before adding the samples, cells were washed for three times with PBS. Then, 100 μl of PEI 25 kDa, PSH, PSH-LP, or TPSH-LP in medium without FBS were added at various concentrations from 0.5 μg/ml to 8 μg/ml. After incubation for 4 h, transfection media was removed and the cells were incubated in fresh DMEM for an additional 20 h. Then, each well was incubated with 20 μl MTT solution (5 mg/ml in PBS) for 4 h. The medium was removed and 100 μl/well of DMSO was added to dissolve the emergent formazan crystals. The optical density was measured at 570 nm in a plate reader. The results were converted into % viability and the mean±SD of 6 replicates for each sample were calculated.

Cellular uptake of LPs. HepG2 cells were plated on 24 well plates at a density of 1×10^5 cells/well and cultivated overnight in 1 ml of DMEM medium containing 10% FBS. The medium was then removed, PBS was added to wash the cells three times and fresh serum-free DMEM medium was added. LOR-2501 5'-labeled with Cy3 (Cy3L) was formulated in the LPs. HepG2 cells were treated with Cy3L-PEI, Cy3L-PSH-LP or Cy3L-TPSH-LP for 4 h. The cells were washed with PBS, digested and fixed in 4% paraformaldehyde solution for 24 h. Cy3L positive HepG2 cells were determined by EPICS XL flow cytometer (Beckman Coulter Corp., Tokyo, Japan). Untreated cells were used as negative control. Each sample was tested by 3 serial measurements at a minimum.

Visualization of internalization of LPs by confocal microscopy. HepG2 cells were seeded in a glass bottom cell culture dish at a density of 1×10^5 cells/well for 24 h. LOR-2501 was labeled with 5'-Cy3 (Cy3L) was mixed with LPs, and the cells were treated with naked Cy3L, Cy3L-PSH-LP, or Cy3L-TPSH-LP for 4 h at 37˚C. Cells were washed 3 times with PBS and fixed in 4% paraformaldehyde for 10 min. Cellular nuclei were stained with DAPI (2 μg/ml) for 3 min followed by washing 3 times with PBS. The cells were observed by Zeiss 710 LSMNLO Confocal Microscope (Carl Zeiss; Jena, Germany).

Determination of R1 protein expression. The expression of R1 protein was assayed using Western blot. Briefly, HepG2 cells were plated on 6 well plates at a density of 1×10^5 cells/well for 24 h. Cells were treated with L-PEI, L-PSH-LP, or L-TPSH-LP for 4 h. The medium

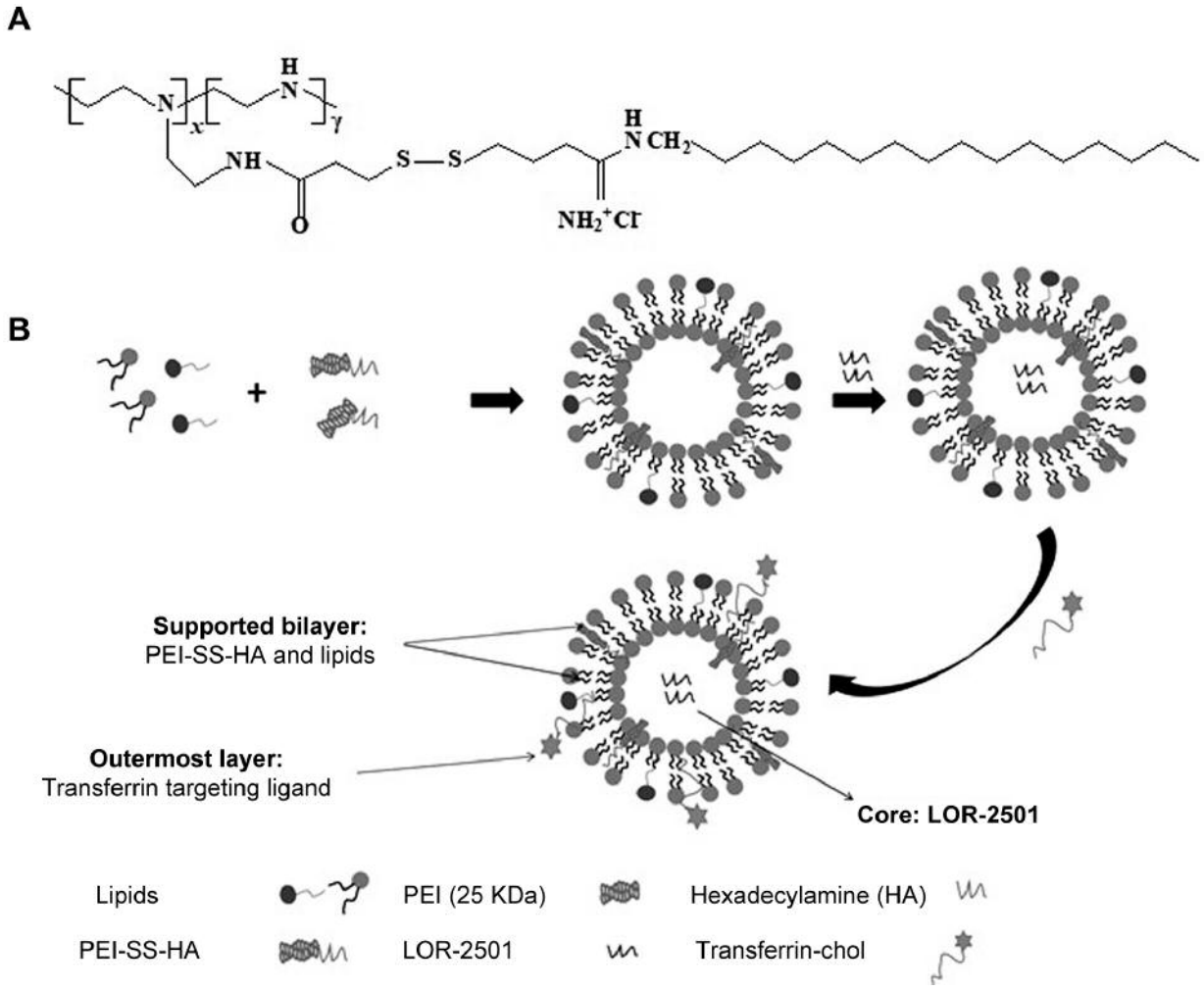

Figure 1. *The proposed structure of PSH and schematic diagram of the preparation process of LPs. (A) The structure of PSH polymer; (B) The schematic diagram of the preparation process of L-PSH-LP and L-TPSH-LP.*

was removed and the cells were cultured for an additional 44 h. The cells were homogenized in RIPA buffer (Sigma) supplemented with 2% PMSF and 1% protease inhibitor cocktail (Sigma). The homogenates were then centrifuged at 10,000 rpm for 5 min at 4˚C. The protein was collected and quantified by Bradford protein assay. Next, 40 μg protein samples were separated by 10% SDS-PAGE gel for electrophoresis and transferred onto PVDF membrane. The membrane was blocked with 5% BSA for 3 h and immunoblotted using primary antibodies to GAPDH or R1 (Abcam Inc., Cambridge, MA, USA) at 4˚C overnight, followed by incubation with horseradish peroxidase-conjugated goat anti-rabbit IgG (Santa Cruz, Santa Cruz, CA, USA) for 4 h at 4˚C. Chemiluminescence was detected using ECL detection kits (GE Healthcare, Waukesha, WI, USA). The intensity of bands was quantified by scanning densitometry using software Quantity one-4.5.0.

Statistical analysis. All the data were expressed as mean±standard deviation (SD). The identification of significant differences between groups was carried out with *t*-test. $p<0.05$ stands for significant difference while $p<0.01$ indicates a highly significant difference.

Results

Formulation and optimization of L-PSH-LP. PEI-SS-HA (PSH) was synthesized based on PEI 25 kDa (Figure 1A), and L-PSH-LP was prepared by the ethanol dilution method (Figure 1B). The particle size and zeta potential of L-PSH-LP at various N/P ratios were measured, and the results are shown in Figure 2A and Figure 2B. As N/P ratios increased from 1:1 to 10:1, particle size first decreased and then increased. The minimum particle size of L-PSH-LP in diameter was 273.03±21.46 nm at N/P of 6:1. At N/P ratios greater than 6:1, the amount of PSH-LP gradually increased. Figure 2B shows that zeta potential changed from negative to positive as the N/P ratio increased. At N/P ratio at 6:1, the zeta potential of the particle reached a plateau, and the value was 15.57±0.82 mV.

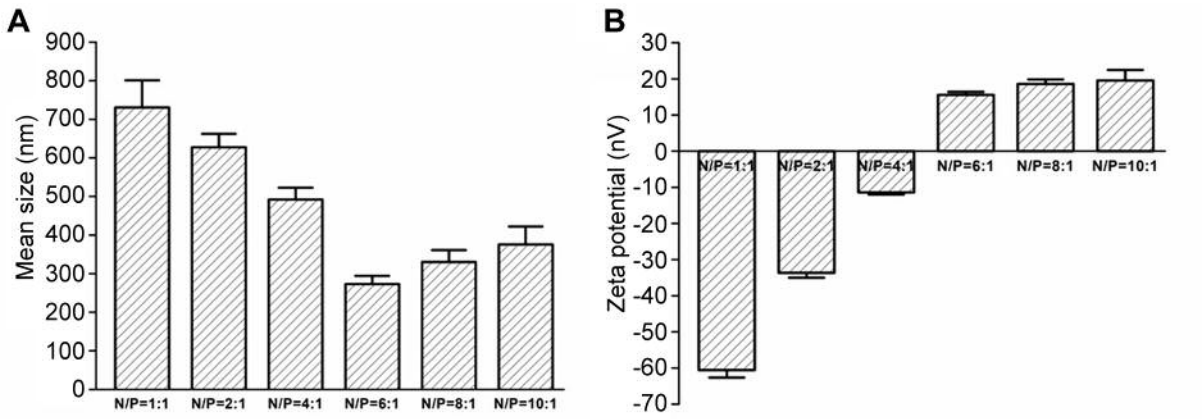

Figure 2. *Mean size and zeta potential of L-PSH-LP at various N/P ratios. (A) Mean size of L-PSH-LP at various N/P ratios; (B) Zeta potential of L-PSH-LP at various N/P ratios from 1:1 to 10:1. Error bars represent standard deviation.*

Characterization of L-TPSH-LP. The particle size and zeta potential of L-TPSH-LP at various Tf-Chol/total lipid ratios were studied to obtain the optimum concentration of Tf-Chol in the LP. Results are shown in Figure 3A and Figure 3B. When the Tf-Chol/total lipid ratio was 1:100, the average particle size of L-TPSH-LP was 267.77±16.20 nm. As the ratio of Tf increased, the zeta potential of L-TPSH-LP decreased, because of the negative charge of the targeting ligand Tf. The average zeta potential of L-TPSH-LP was 4.87±0.52 mV when the Tf-Chol/total lipid ratio was 1:100, which is appropriate for cellular uptake by cancer cells. Figure 3C shows the diameter distribution of L-TPSH-LP at Tf-Chol/total lipid ratio of 1:100. The structure of the L-TPSH-LP at Tf-Chol/total lipid ratio of 1:100 was observed under SEM. The results are shown in Figure 3D. The SEM image showed that the L-TPSH-LP has a spherical morphology, and the particle size of L-TPSH-LP is about 200 nm, which is consistent with the results of particle size measurement.

Buffer capacity determination of PSH and agarose gel electrophoresis retardation assay of LPs. Figure 4A shows the results of the buffer capacity of H2O, PEI 25 kDa, and PSH. In the process of titration, the pH values of water changed rapidly from 10 to 3 with the addition of HCl solution, while the pH curve of PEI 25 kDa and PSH solutions presented a stable downward trend, which indicates the proton sponge effect of PEI, which may facilitate intracellular oligo delivery.

In order to further evaluate the formation of complexes between LPs and LOR-2501, an agarose gel electrophoresis retardation assay was carried out. In the experiment, the naked LOR-2501 was used as a control. The results are shown in Figure 4B. The naked LOR-2501 showed a bright band in the gel. However, no bright bands in the lanes of L-PEI, L-PSH-LP at the N/P ratios of 6:1, 8:1 and 10:1, and L-TPSH-LP were visible. Results showed that PSH-LP and TPSH-LP were able to completely retard LOR-2501 to form nanoparticles.

Cytotoxicity of polymers and LPs. HepG2 cells were treated with PEI 25 kDa, PSH, PSH-LPm or TPSH-LP. Untreated HepG2 cells were used as a control. The concentrations of PEI 25 kDa, PSH, PSH-LP, or TPSH-LP were from 0.5~8μg/ml. Viabilities of HepG2 cells are shown in Figure 5. PSH had no significant cytotoxicity to HepG2 cells, and the cell viability was above 85% at the tested concentrations. However, PEI 25 kDa reduced cell viability to 49.11% at the concentration of 8 μg/ml. The toxicity of PSH was reduced compared with PEI. This was because a large number of amino groups in PEI were replaced. PSH showed low toxicity compared with PEI itself, which was highly desirable. In the case of PSH-LP and TPSH-LP, cell viabilities of HepG2 cells were all above 90%. Therefore, both PSH-LP and TPSH-LP could safely be used as vectors to deliver LOR-2501.

Cellular uptake of LOR-2501 delivered by LPs. Flow cytometry was firstly used to analyze the effect of LPs on the uptake of LOR-2501 in HepG2 cells. As shown in Figure 6A and Figure 6B, the uptake of Cy3L-PSH-LP was much higher than those complexed to PEI 25 kDa. The increase was even greater than Cy3L-PSH-LP when Cy3L-TPSH-LP was used, which showed the ligand Tf could improve the uptake of LP. The mean fluorescence intensities of HepG2 cells were also obtained, the trend was consistent with Figure 6A. The mean fluorescence intensity value in the case of Cy3L-TPSH-LP was about 3 times that of Cy3L-PEI and 2 times that of Cy3L-PSH-LP. These results indicated that TPSH-LP was more effective for *in vitro* delivery of LOR-2501.

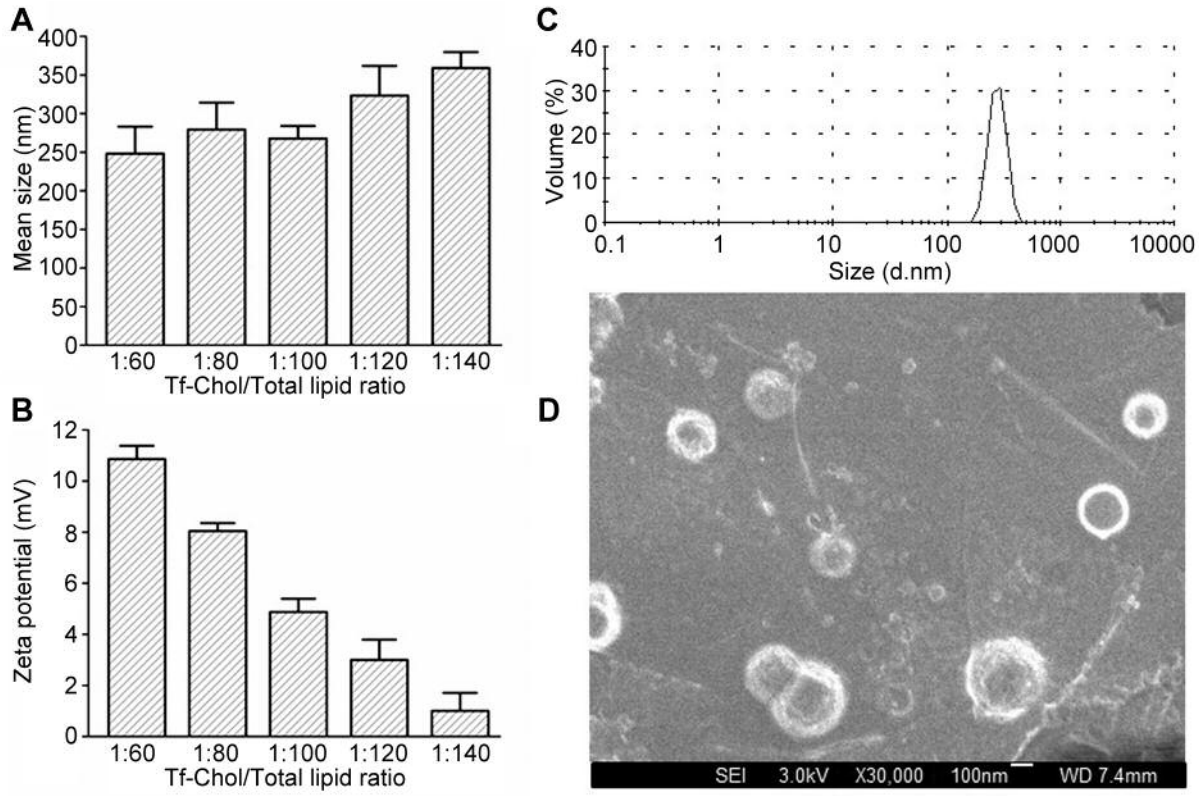

Figure 3. *Characterization of L-TPSH-LP. (A) Mean size of L-TPSH-LP at various Tf-Chol/total lipid ratios; (B) zeta potential of L-TPSH-LP at various Tf-Chol/total lipid ratios; (C) diameter distribution of L-TPSH-LP at Tf-Chol/total lipid ratio 1:100; (D) SEM image of L-TPSH-LP at Tf-Chol/total lipid ratio 1:100.*

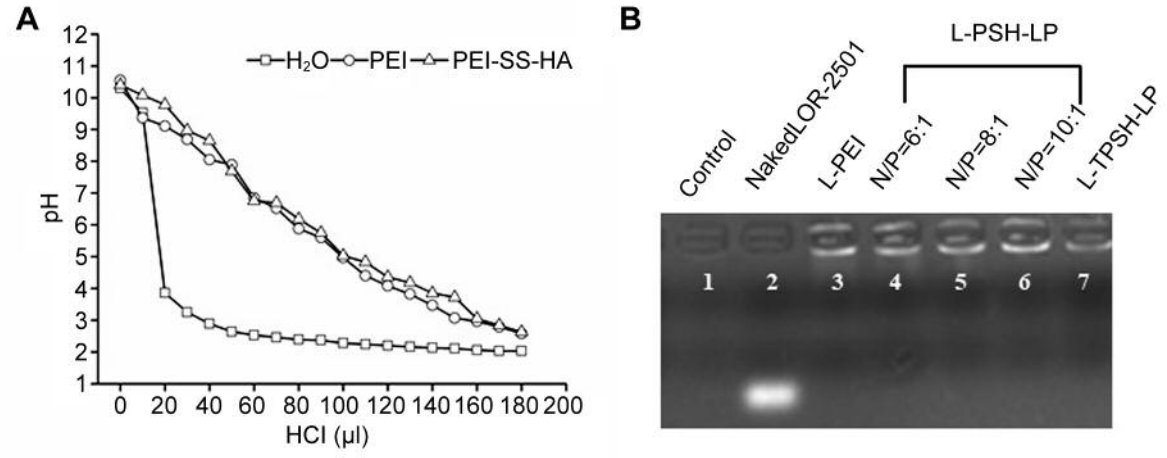

Figure 4. *Buffer capacity determination of the polymers and agarose gel electrophoresis retardation assay of the LPs. (A) Buffer capacity determination of H_2O, PEI 25 kDa and PSH by acid-base titration; (B) agarose gel electrophoresis retardation assay of L-PSH-LP and L-TPSH-LP.*

The R1 protein levels in the LPs-treated HepG2 cells were determined by western blot analysis (Figure 6C and Figure 6D). Delivery of LOR-2501 in HepG2 cells by L-PEI, L-PSH-LP, or L-TPSH-LP resulted in R1 downregulation to 25.80%, 45.71% and 64.15%, respectively. Compared to L-PEI and L-PSH-LP, L-TPSH-LP showed statistically significant down regulation ($p<0.05$).

Intracellular localization of LPs. HepG2 cells were treated with naked Cy3L, Cy3L-PSH-LP or Cy3L-TPSH-LP, and the

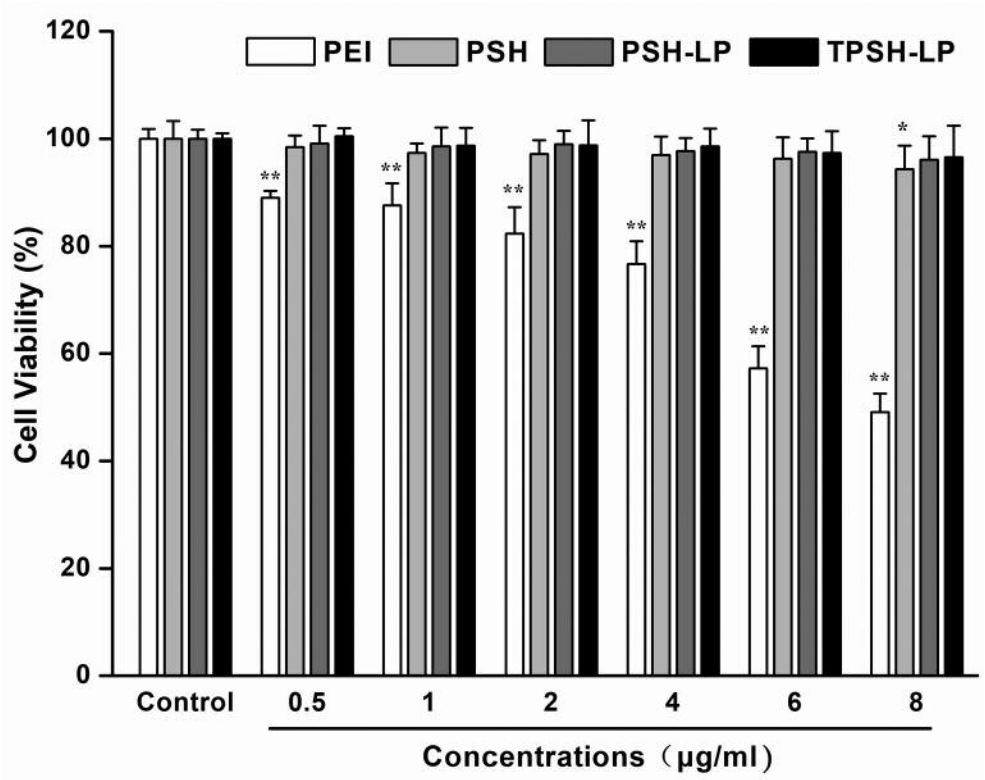

Figure 5. *Cytotoxicity tests of the polymers and LPs in HepG2 cells. Viabilities of HepG2 cells treated with PEI 25 kDa, PSH, PSH-LP, and TPSH-LP at various concentrations were measured by the MTT assay. Untreated cells were used as a control. Each bar is the mean of six experiments normalized to mean±SD. (*p<0.05 vs. control, **p<0.01 vs. control).*

intracellular distribution of LOR-2501 was directly observed by confocal microscopy (Figure 7). Compared to naked Cy3L, Cy3L-PSH-LP and Cy3L-TPSH-LP was internalized by HepG2 cells more efficiently, and the fluorescence intensity of cells treated with Cy3L-TPSH-LP was much higher than those treated with Cy3L-PSH-LP. Most of Cy3L accumulated in the cytoplasm or around the nucleus of HepG2 cells, which suggested that LOR-2501 delivered by L-PSH-LP and especially L-TPSH-LP could enter into the cytoplasm and the nucleus.

Discussion

The development of high-efficient and safe oligonucleotide delivery carriers remains a challenge. PEI 25 kDa is one of the most potent gene delivery vectors because of its "proton sponge" effect. However, clinical use of PEI 25 kDa is limited due to its high cytotoxicity and the lack of targeting. Our previous findings suggest that hydrophobic modification of PEI 25 kDa could improve its delivery activity and reduce the toxicity. However, the targeting efficiency still needed to be improved (18, 20). In this study, a reduction-sensitive cationic polymer PEI-SS-HA (PSH) based on PEI 25 kDa was synthesized. PSH was combined with lipids and transferrin (Tf) to form the nanoparticle TPSH-LP, which was used to delivery LOR-2501. The properties of TPSH-LP, including cytotoxicity, cellular uptake and R1 silencing in HepG2 cells were investigated.

In the process of forming the delivery system, the ratio between the LPs and LOR-2501 needed to be optimized (25, 26). So, the N/P ratios of L-PSH-LP were firstly optimized. At the optimal N/P ratio of 6:1 the particle size of L-PSH-LP in diameter was 273.03±21.46 nm, and the zeta potential value was 15.57±0.82 mV (Figure 2A and B).

For the purpose of increasing targeting delivery, Tf was conjugated at the outermost layer of the LPs. TPSH-LP had a spherical morphology, and the particle size of L-TPSH-LP was about 200 nm (Figure 3C and D). The proton sponge effect is important for endosomal release of oligos. Therefore, the measurement of buffer capacity is important for PEI and the modified PEI (PSH). Results showed that PSH had a high buffering capacity (Figure 4A). Agarose gel electrophoresis retardation assay was used to further evaluate the binding of LPs and LOR-2501. Results showed that PSH-LP and TPSH-LP were able to completely retard LOR-2501 by forming nanoparticles (Figure 4B). Cytotoxicity

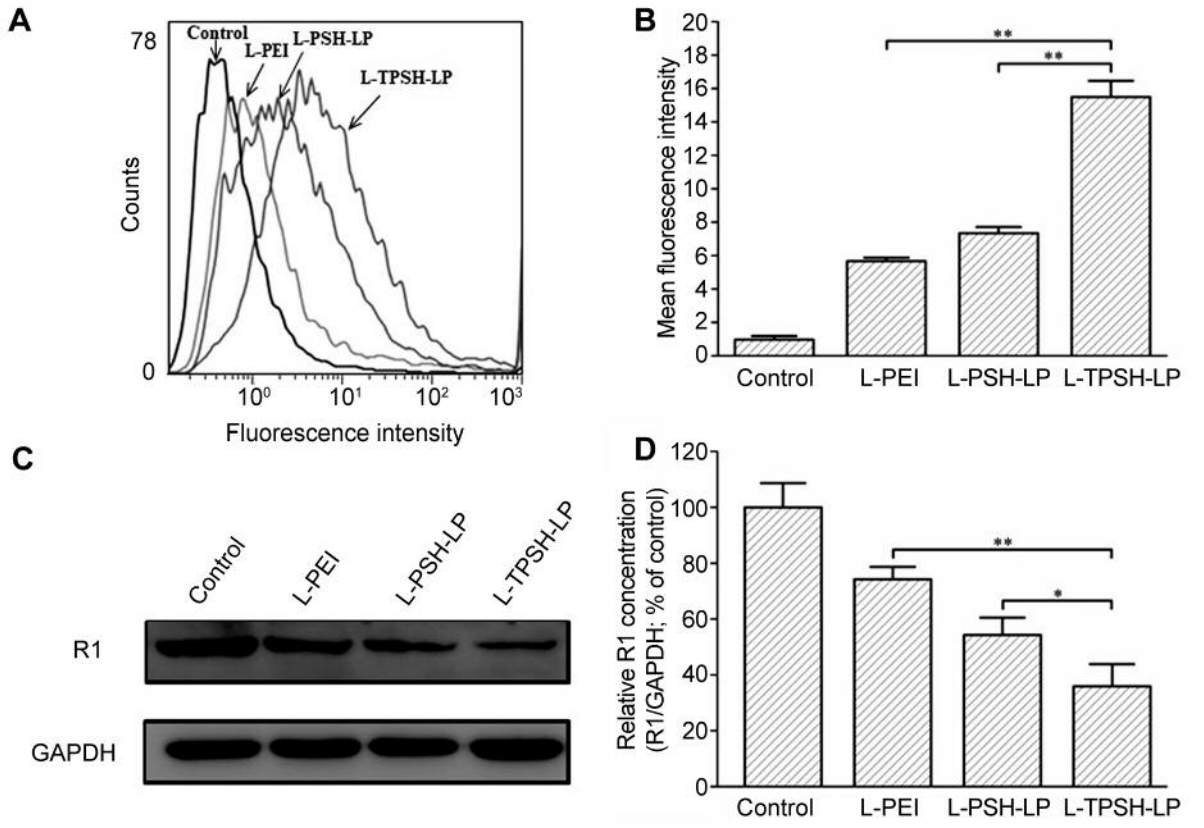

Figure 6. *Cellular uptake of LOR-2501 delivered by LPs. (A) Flow cytometric assay of the cellular fluorescence uptake in HepG2 cells treated with LOR-2501 labeled with 5'-Cy3 (Cy3L), Cy3L-PEI, Cy3L-PSH-LP, and Cy3L-TPSH-LP; (B) the mean fluorescence values of HepG2 cells; (C) down-regulation of R1 protein in HepG2 cells expression by western blot; (D) densitometric analysis of the bands. Each bar is the mean±SD of three experiments. (*p<0.05, **p<0.01).*

tests of polymers and LPs showed that PSH, PSH-LP, and TPSH-LP had no significant cytotoxicity towards HepG2 cells, and cell viability was above 85% at the tested concentrations (Figure 5).

Data also indicated that TPSH-LP was more effective for the delivery of LOR-2501. The mean fluorescence intensity value in the case of Cy3L-TPSH-LP was about 3 times that of Cy3L-PEI and 2 times that of L-PSH-LP/LOR-2501 (Figure 6A and B). Treatment of HepG2 cells with Cy3L-TPSH-LP resulted in R1 down-regulation to 64.15% in (Figure 6C and D). Therefore, adding of Tf was effective in increasing delivery efficiency of LOR-2501. TPSH-LP could help LOR-2501 to enter into HepG2 cells more efficiently than others and reduce the expression of R1 protein, which was closely related to the growth and differentiation of tumor cells during transcription and translation (27).

The uptake of Cy3L-PSH-LP and Cy3L-TPSH-LP by HepG2 cells was also investigated by confocal laser scanning microscopy. Cy3L delivered by the Cy3L-PSH-LP and especially Cy3L-TPSH-LP could enter into the cytoplasm and even the nucleus (Figure 7). The results indicated that TPSH-LP delivers higher levels of LOR-2501 than PEI and PSH-LP. The incorporation of Tf might promote uptake by HepG2 cells *via* Tf receptors (28).

In conclusion, a novel reduction-sensitive cationic polymer was synthesized based on PEI 25 kDa, PEI-SS-HA (PSH). PSH showed reduced toxicity compared with PEI 25 kDa. Meanwhile, PSH had high buffering capacity and can be targeted for internalization using Tf. The obtained LPs were used to deliver LOR-2501. L-TPSH-LP was demonstrated to have high delivery activity *in vitro*. The particle size and zeta potential of L-TPSH-LP were suitable for the delivery to tumor cells. TPSH-LP was able to transport LOR-2501 to tumor cells safely and efficiently. Therefore, L-TPSH-LP may be suitable and effective for future clinical applications.

Conflicts of Interest

The Authors declare no conflicts of interest regarding this study.

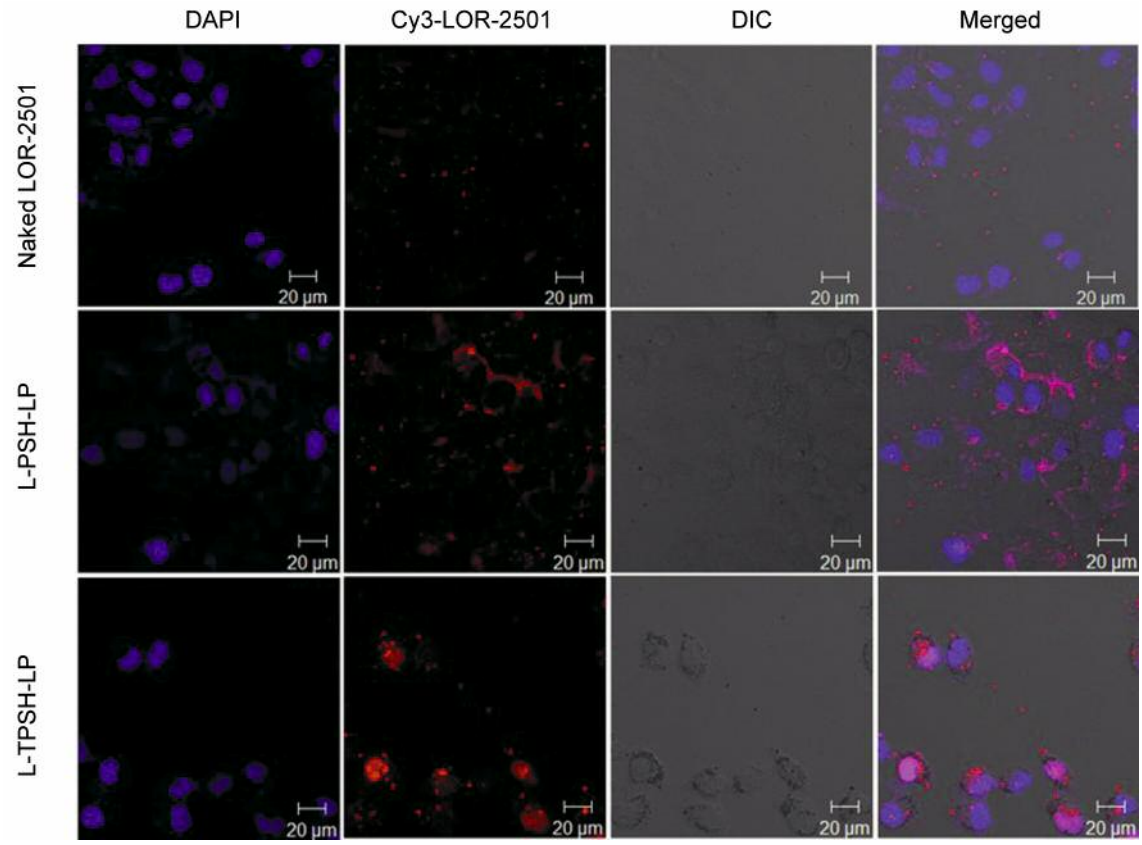

Figure 7. *Intracellular localization of LPs in HepG2 cells shown by confocal microscopy. 5'-Cy3 fluorescence is shown in red, DAPI nuclear staining is shown in blue. Scale bar=20 μm.*

Acknowledgements

This research was funded by Startup Foundation for Doctors of Shanxi Medical University (No. BS03201621 and No. BS03201608) and the Fund for Shanxi Key Subjects Construction (FSKSC).

Authors' Contributions

Conceptualization: Bin Zheng and Shuang Yang; experimental design: Bin Zheng, Shuang Yang and Yin Xie; data analysis: Shuang Yang; experimentation, Bin Zheng, Shuang Yang, and Qingping Tian; data compilation: Bin Zheng; manuscript preparation – original draft: Shuang Yang; review and editing: Shuqiu Zhang and Robert J. Lee; supervision: Shuqiu Zhang and Robert J. Lee; project administration: Bin Zheng and Shuqiu Zhang.

References

1 Yang S, Yang X, Liu Y, Zheng B, Meng L, Lee RJ, Xie J and Teng L: Non-covalent complexes of folic acid and oleic acid conjugated polyethylenimine: An efficient vehicle for antisense oligonucleotide delivery. Colloids Surf B Biointerfaces *135*: 274-282, 2015. PMID: 26263216. DOI: 10.1016/j.colsurfb.2015. 07.047

2 Lee Y, Vassilakos A, Feng N, Jin H, Wang M, Xiong K, Wright J and Young A: GTI-2501, an antisense agent targeting R1, the large subunit of human ribonucleotide reductase, shows potent anti-tumor activity against a variety of tumors. Int J Oncol *28*: 469-478, 2006. PMID: 16391803.

3 Yang Z, Yu B, Zhu J, Huang X, Xie J, Xu S, Yang X, Wang X, Yung BC, Lee LJ, Lee RJ and Teng L: A microfluidic method to synthesize transferrin-lipid nanoparticles loaded with siRNA LOR-1284 for therapy of acute myeloid leukemia. Nanoscale *6*: 9742-9751, 2014. PMID: 25003978. DOI: 10.1039/c4nr01510j

4 Yang Z, Gao D, Cao Z, Zhang C, Cheng D, Liu J and Shuai X: Drug and gene co-delivery systems for cancer treatment. Biomater Sci *3*: 1035-1049, 2015. PMID: 26221938. DOI: 10.1039/c4bm00369a

5 Scheicher B, Schachner-Nedherer AL and Zimmer A: Protamine-oligonucleotide-nanoparticles: Recent advances in drug delivery and drug targeting. Eur J Pharm Sci *75*: 54-59, 2015. PMID: 25896372. DOI: 10.1016/j.ejps.2015.04.009

6 Ezzat K, Aoki Y, Koo T, McClorey G, Benner L, Coenen-Stass A, O'Donovan L, Lehto T, Garcia-Guerra A, Nordin J, Saleh AF, Behlke M, Morris J, Goyenvalle A, Dugovic B, Leumann C, Gordon S, Gait MJ, El-Andaloussi S and Wood MJ: Self-assembly into nanoparticles is essential for receptor mediated uptake of therapeutic antisense oligonucleotides. Nano Lett *15*: 4364-4373,

2015. PMID: 26042553. DOI: 10.1021/acs.nanolett.5b00490
7 Harmsen S, Wall MA, Huang R and Kircher MF: Cancer imaging using surface-enhanced resonance Raman scattering nanoparticles. Nat Protoc *12*: 1400-1414, 2017. PMID: 2868 6581. DOI: 10.1038/nprot.2017.031
8 Yingchoncharoen P, Kalinowski DS, and Richardson DR: Lipid-based drug delivery systems in cancer therapy: What is available and what is yet to come. Pharmacol Rev *68*: 701-787, 2016. PMID: 27363439. DOI: 10.1124/pr.115.012070
9 Du C, Yan H, Liang J, Luo A, Wang L, Zhu J, Xiong H and Chen Y: Polyethyleneimine-capped silver nanoclusters for microRNA oligonucleotide delivery and bacterial inhibition. Int J Nanomedicine *12*: 8599-8613, 2017. PMID: 29238194. DOI: 10.2147/IJN.S146968
10 Jiang D, Wang M, Wang T, Zhang B, Liu C and Zhang N: Multifunctionalized polyethyleneimine-based nanocarriers for gene and chemotherapeutic drug combination therapy through one-step assembly strategy. Int J Nanomedicine *12*: 8681-8698, 2017. PMID: 29263663. DOI: 10.2147/IJN.S142966
11 Ko YT, Kale A, Hartner WC, Papahadjopoulos-Sternberg B and Torchilin VP: Self-assembling micelle-like nanoparticles based on phospholipid-polyethyleneimine conjugates for systemic gene delivery. J Control Release *133*: 132-138, 2009. PMID: 18929605. DOI: 10.1016/j.jconrel.2008.09.079
12 Ahmadzada T, Reid G and McKenzie DR: Fundamentals of siRNA and miRNA therapeutics and a review of targeted nanoparticle delivery systems in breast cancer. Biophys Rev *10*: 69-86, 2018. PMID: 29327101. DOI: 10.1007/s12551-017-0392-1
13 Kapadia CH, Tian S, Perry JL, Luft JC and DeSimone JM: Reduction sensitive PEG hydrogels for codelivery of antigen and adjuvant to induce potent CTLs. Mol Pharm *13*: 3381-3394, 2016. PMID: 27551741. DOI: 10.1021/acs.molpharmaceut.6b00288
14 Lei Q, Hu JJ, Rong L, Cheng H, Sun YX, and Zhang XZ: Gold nanocluster decorated polypeptide/DNA complexes for NIR light and redox dual-responsive gene transfection. Molecules *21*, 2016. PMID: 27556436. DOI: 10.3390/molecules21081103
15 Dong J, Cao Y, Shen H, Ma Q, Mao S, Li S and Sun J: EGFR aptamer-conjugated liposome-polycation-DNA complex for targeted delivery of SATB1 small interfering RNA to choriocarcinoma cells. Biomed Pharmacother *107*: 849-859, 2018. PMID: 30142547. DOI: 10.1016/j.biopha.2018.08.042
16 Xing H, Hwang K and Lu Y: Recent developments of liposomes as nanocarriers for theranostic applications. Theranostics *6*: 1336-1352, 2016. PMID: 27375783. DOI: 10.7150/thno.15464
17 Yuan Y, Zhang L, Cao H, Yang Y, Zheng Y and Yang XJ: A polyethylenimine-containing and transferrin-conjugated lipid nanoparticle system for antisense oligonucleotide delivery to AML. Biomed Res Int *2016*: 1287128, 2016. PMID: 27034925. DOI: 10.1155/2016/1287128
18 Yang S, Guo Z, Yang X, Xie J, Lee RJ, Jiang D and Teng L: Enhanced survivin siRNA delivery using cationic liposome incorporating fatty acid-modified polyethylenimine. Chem Res Chinese U *31*: 401-405, 2015. DOI: 10.1007/s40242-015-5060-z
19 Opanasopit P, Paecharoenchai O, Rojanarata T, Ngawhirunpat T and Ruktanonchai U: Type and composition of surfactants mediating gene transfection of polyethylenimine-coated liposomes. Int J Nanomedicine *6*: 975-983, 2011. PMID: 21720509. DOI: 10.2147/IJN.S18647
20 Yang S, Lee RJ, Yang X, Zheng B, Xie J, Meng L, Liu Y and Teng L: A novel reduction-sensitive modified polyethylenimine oligonucleotide vector. Int J Pharm *484*: 44-50, 2015. PMID: 25698089. DOI: 10.1016/j.ijpharm.2015.02.036
21 Wang Y, Chen P and Shen J: The development and characterization of a glutathione-sensitive cross-linked polyethylenimine gene vector. Biomaterials *27*: 5292-5298, 2006. PMID: 16806454. DOI: 10.1016/j.biomaterials.2006.05.049
22 Li Y, Lee RJ, Yu K, Bi Y, Qi Y, Sun Y, Xie J and Teng L: Delivery of siRNA using lipid nanoparticles modified with cell penetrating peptide. ACS Appl Mater Interfaces *8*: 26613-26621, 2016. PMID: 27617513. DOI: 10.1021/acsami.6b09991
23 Feng T, Wei Y, Lee RJ and Zhao L: Liposomal curcumin and its application in cancer. Int J Nanomedicine *12*: 6027-6044, 2017. PMID: 28860764. DOI: 10.2147/IJN.S132434
24 Koh CG, Zhang X, Liu S, Golan S, Yu B, Yang X, Guan J, Jin Y, Talmon Y, Muthusamy N, Chan KK, Byrd JC, Lee RJ, Marcucci G and Lee LJ: Delivery of antisense oligodeoxyribonucleotide lipopolyplex nanoparticles assembled by microfluidic hydrodynamic focusing. J Control Release *141*: 62-69, 2010. PMID: 19716852. DOI: 10.1016/j.jconrel.2009.08.019
25 Bofinger R, Zaw-Thin M, Mitchell NJ, Patrick PS, Stowe C, Gomez-Ramirez A, Hailes HC, Kalber TL and Tabor AB: Development of lipopolyplexes for gene delivery: A comparison of the effects of differing modes of targeting peptide display on the structure and transfection activities of lipopolyplexes. J Pept Sci *24*: e3131, 2018. PMID: 30325562. DOI: 10.1002/psc.3131
26 Ewe A, Panchal O, Pinnapireddy SR, Bakowsky U, Przybylski S, Temme A and Aigner A: Liposome-polyethylenimine complexes (DPPC-PEI lipopolyplexes) for therapeutic siRNA delivery in vivo. Nanomedicine-Uk *13*: 209-218, 2017. PMID: 27553077. DOI: 10.1016/j.nano.2016.08.005
27 Chen Y, Huang Y, Chen DM, Wu C, Leng QP, Wang WY, Deng MQ, Zhao YX and Yang XH: RRM1 expression and the clinicopathological characteristics of patients with non-small cell lung cancer treated with gemcitabine. Onco Targets Ther *11*: 5579-5589, 2018. PMID: 30237724. DOI: 10.2147/OTT.S162667
28 Bi Y, Lee RJ, Wang X, Sun Y, Wang M, Li L, Li C, Xie J and Teng L: Liposomal codelivery of an SN38 prodrug and a survivin siRNA for tumor therapy. Int J Nanomedicine *13*: 5811-5822, 2018. PMID: 30323583. DOI: 10.2147/IJN.S173279

Received February 16, 2019
Revised March 10, 2019
Accepted March 13, 2019